

Polystyrenes with macro-intercalated organoclay. Part I. Compounding and characterization

Maryam Sepehr^a, Leszek A. Utracki^{a,*}, Xiaoxia Zheng^b, Charles A. Wilkie^b

^a Industrial Materials Institute, National Research Council Canada, 75 de Mortagne, Boucherville, Que., Canada J4B 6Y4

^b Department of Chemistry, Marquette University, P.O. Box 1881, Milwaukee, WI 53201, USA

Received 23 August 2005; received in revised form 27 September 2005; accepted 1 October 2005

Available online 24 October 2005

Abstract

Nanocomposites of polystyrene (PS) were prepared using a melt compounding or co-solvent method. Two commercial PS were used, and two organoclays—one prepared in this laboratory (COPS), and the other commercial Cloisite® 10A (C10A). The COPS is a product of clay intercalation with a copolymer of styrene and vinyl benzyl tri-methyl ammonium chloride. According to the XRD diffraction data, the clay platelets in COPS and its PNC with PS were relatively well dispersed, i.e. with the interlayer spacings of $d_{001} = 7\text{--}8$ nm. By contrast, d_{001} in PNC prepared with C10A was only 4 nm. However, the number of clay platelets per stack in PS/COPS was found to be significantly larger than that in PS/C10A, viz. $m = 3\text{--}12$, compared to $m = 2\text{--}6$. The scanning and transmission electron microscopy indicated that in the PS matrix COPS existed in form of large, immiscible domains.

© 2005 Elsevier Ltd. All rights reserved.

Keywords: Polystyrene; Nanocomposites; Phase separation

1. Introduction

Polymer/clay nanocomposites (PNC) consist of inorganic layered clay dispersed in a polymeric matrix. To maximize the effect of nano-filler on performance it is important that the clay is exfoliated. This may be accomplished in two steps: (i) clay intercalation by an organic modifier, and (ii) exfoliation of the intercalated clay either during polymerization (reactive exfoliation), during mechanical compounding in a melt mixer (mechanical exfoliation), or using a common solvent for organoclay and the matrix polymer.

In systems containing nanometer size particles, the total interfacial area is large (the specific surface area of montmorillonite, MMT, is about $750\text{ m}^2/\text{g}$). Since MMT platelets have large aspect ratios (e.g. $p \equiv \text{diameter/thickness} \cong 100\text{--}300$), at loadings $w > 1.2\text{ wt}\%$ their encompassed volumes starts to overlap, hindering the free rotation, and random distribution; hence exfoliation. Thus, at higher clay concentrations a local ordering of platelets is expected and the motion of polymer molecules restricted. This is the basic

reason why incorporation of a small amount of nanometer-size clay platelets leads to the excellent performance of PNC; the mechanical and thermal properties of a polymer can be significantly improved, as well as gas barrier, flame retardancy, moldability, surface finish, etc. [1,2].

The mechanical exfoliation of PNC is usually accomplished by melt compounding an organoclay with a polymeric matrix. The key to success is miscibility of the intercalant with the polymeric matrix, and its thermal stability under the processing conditions. Exfoliation of clay platelets by polar polymers with groups capable of strong interactions with the clay platelets (e.g. polyamide) is relatively easy. By contrast, it is much more difficult to exfoliate clay in a nonpolar polymer such as polypropylene (PP), or polystyrene (PS). Often it is necessary to use a compatibilizer to enhance miscibility.

Development of PS-based nanocomposites is important from the industrial and academic points of view; it is a major commodity polymer, and being amorphous it is expected to generate model PNC for studies of the clay content vs. performance relationships. However, so far melt compounding of PS with organoclay did not result in a controlled degree of clay dispersion. By contrast, exfoliation has been achieved in reactive processes. Polymerization in the presence of non-reactive organoclay has been carried out in bulk (using free radical or coordination method), as well as in emulsion, suspension, or solution [2,3]. The reaction usually results in

* Corresponding author. Tel.: +1 450 641 5182; fax: +1 450 641 5105.

E-mail address: leszek.utracki@cnrc_nrc.gc.ca (L.A. Utracki).

high degree of clay dispersion. However, there are several disadvantages: (1) the reaction is slow (it may take more than 24 h), (2) exfoliation is not thermodynamically stable and the platelets re-aggregate during subsequent processing or forming steps, and (3) the process is available only to the resin manufacturer who is able to dedicate a production line for this purpose (clay is catalytically active). To bypass problems 1 and 2, PS-based PNC were prepared starting with organoclay pre-intercalated with a vinyl-terminated reactive compound, viz. vinyl benzyl di-methyl dodecyl ammonium chloride [4,5], vinyl tri-ethoxy silane (used with cetyl pyridinium chloride) [4], vinyl benzyl di-methyl ethanol ammonium chloride [6], the quaternized reaction product of azo-bis [methyl-*N*-(2-ethoxy) propionamide] with bromo acetyl bromide [7], [2-(acryloyloxy)ethyl](4-benzoylbenzyl)di-methyl ammonium bromide [8], or tri-methyl-*N*-methyl-styrene [9]. After polymerization, PNC with a high degree of exfoliation was obtained; the dispersion of the end-tethered clay platelets was stable.

Mechanical exfoliation has several advantages: (1) it is rapid (<10 min), (2) it is controlled by the thermodynamic interactions, thus there is no danger of re-aggregation during the forming stage, and (3) the process is available to anyone having a suitable compounding line. The main disadvantage is the need for miscible with PS, and a thermally stable (at the processing conditions) organoclay. The mathematical modeling of the free energy changes during intercalation leads to the conclusion that the most effective organoclays are these that contain macromolecular intercalant [10,11].

During the last few years many research groups studied the melt intercalation/exfoliation of PS/clay systems. Hasegawa et al. [12] produced partially exfoliated PS-clay nanocomposites by compounding in a twin-screw extruder (TSE) 7 wt% of organoclay with an immiscible blend of PS and $\geq 50\%$ of a compatibilizer. The organoclay was MMT pre-intercalated with trimethyl octadecyl ammonium chloride (3MODA), while the compatibilizer was poly(styrene-*co*-methyl vinyl oxazoline). Hoffmann et al. [13] used synthetic fluoromica (FM) pre-intercalated with either 2-phenylethylamine (PEA) or with amine-terminated polystyrene (AT-PS; $M_n = 5.8$ kg/mol).

The authors prepared PNC by compounding PS with 5 wt% of organoclay at 200 °C in a micro-compounder. According to XRD, the PNC with PEA did not intercalate ($d_{001} = 1.4$ nm), but in the one prepared with the end-tethered AT-PS the clay platelets were highly dispersed ($d_{001} > 4$ nm); the observation was confirmed by TEM.

Several companies manufacture organoclay on the industrial scale. These commercial organoclays have been used by various researchers for the preparation of PS-clay nanocomposite by melt compounding in the extruder or internal mixer [14–17]. Although intercalation of PS into interlamellar galleries was realized, exfoliation was not achieved.

Yoon et al. [18] reported on the effects of polar comonomers and shear on the performance of PNC with PS matrix. PS and three commercial styrenic copolymers composed of styrene (ST), acrylonitrile (AN) and methylvinyl oxazoline (OZ) were used. The organoclay was MMT intercalated with di-methyl benzyl hydrogenated tallow ammonium chloride (MMT-2MBHTA, Cloisite® 10A; or C10A for short). PNC with 5 wt% of C10A were prepared using either static annealing or compounding in an internal mixer at $T = 210$ °C. Owing to thermal instability of the organoclay, the interlayer spacing initially expanded then decreased from $d_{001} = 3.5$ to 1.9 nm. The effect was moderated by the presence of AN or OZ comonomer. Similarly, mixing of PS with 1–10 wt% of C10A in an internal mixer was carried out at $T = 180$ – 200 °C [17]. The resulting interlayer spacing, $d_{001} \cong 3.6$ nm, was virtually independent of the mixing conditions. The tensile measurements indicated that the presence of organoclay enhanced the modulus by ca. 70%, but reduced the tensile strength. Tanoue et al. melt compounded PS with up to 20 wt% C10A in a co-rotating, intermeshing TSE, under a variety of processing conditions [19–21]. Three grades of PS with different molecular weight were used. The organoclay was dispersed into two types of stacks, with the interlayer spacings of $d_{001} = 4.20$ and 1.6 nm. Since C10A has $d_{001} = 1.93$ nm, the first peak indicated intercalation and the other a collapse of the interlamellar gallery caused by the thermal degradation of the intercalant.

Table 1
Materials characteristics

Material (code)	Supplier	Specification
Organoclay (COPS)	Marquette University	Na-MMT intercalated with a copolymer of styrene with vinylbenzyl tri-methyl ammonium chloride
Organoclay (Cloisite® 10A; C10A) is a Na-MMT ^a intercalated with 2MBHTA ^b	Southern Clay Products, Gonzales, TX	$\begin{array}{c} \text{CH}_3 \\ \\ \text{CH}_3 - \text{N}^+ - \text{CH}_2 - \text{C}_6\text{H}_5 \\ \\ \text{HT} \end{array}$ Organic loading = 1.25 mequiv/g Organic content = 39 wt% Interlayer spacing: $d_{001} = 1.94$ nm MFR ^c = 3.5 g/10 min; $M_w = 270$ kg/mol MFR ^c = 20.3 g/10 min; $M_w = 116$ kg/mol ^d
Polystyrene 1301 (PS-1301)	NOVA Chemicals	
Delltec PS-20.3	Delltec	

^a Na-MMT, cation exchange capacity: (CEC) = 0.926 mequiv/g; interlayer spacing, $d_{001} = 1.17$ nm.

^b 2MBHTA = di-methyl, benzyl hydrogenated tallow ammonium chloride (tallow contains: $\sim 65\%$ C₁₈; $\sim 30\%$ C₁₆; $\sim 5\%$ C₁₄).

^c By ASTM D1238, procedure B; 200/5.0.

^d Estimated from MFR.

Thus, the experience indicates that there are two main obstacles for the preparation of PS-based PNC: immiscibility of the (mainly paraffinic) intercalant with PS matrix, and poor thermal stability of commercial organoclays. Accordingly, the aim of this work is to explore the possibility of using a new class of organoclays, prepared with long-chain intercalant, an oligo-styrene, or COPS.

2. Experimental

2.1. Materials

In this work two commercial PS resins, and two organoclays (C10A, and an experimental one) were used. Their characteristics are given in Table 1.

2.1.1. Preparation of COPS modified clay [22]

A 1 l, 3-neck round bottom flask was charged with: 8.22 g (0.0390 mol) vinyl-benzyl trimethyl ammonium chloride (VBTACl), 208 g (2.00 mol) of inhibitor-free styrene, 21 g of benzoyl peroxide (BPO) and 400 ml solvent (CHCl₃/ETOH = 1/1). The contents of the flask were stirred until all had dissolved at room temperature under flow of N₂. Next, the solution was heated in oil bath to ca. 80 °C under reflux while stirring for 6 h. The mixture was then cooled to room temperature and solvent was evaporated. The resulting solid was dissolved in THF, and then precipitated with methanol, obtaining 205 g of a white solid. The molecular weight (based on the Mark–Houwink–Sakurada constants for PS [23]) was about 5 kg/mol.

A suspension of pre-dispersed Na-MMT (33 g clay and 2.2 l of distilled water) and 1.8 l THF was stirred at room

Table 2
Composition, processing methods, and XRD result for the prepared samples

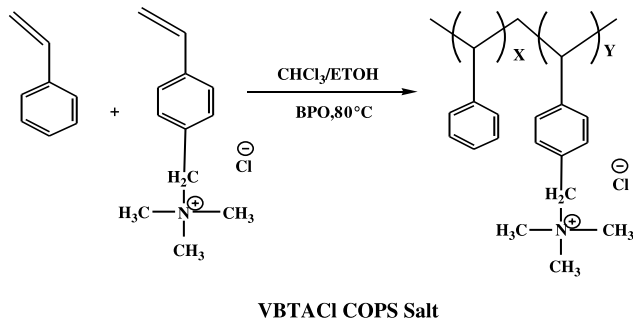
Identification code	Composition				Processing method	Processing parameters				XRD results		
	Grade of PS	Organo-clay	Organo-clay (wt%)	Clay-MMT (wt%)		$t_{\text{backflow-hannel}}$ (min)	Q (kg/h)	T (°C)	N (rpm)	Interlayer spacing (nm) ^a		Number of platelets per stack ^b
										Main	Secondary	
COPS	–	COPS	100	21.7	–	–	–	–	–	8.8	4.5	7.0
C10A	–	C10A	100	61	–	–	–	–	–	1.94	–	1.9
B3	1301	COPS	4.35	0.9	Mini-	0	–	200	100	6.9	3.6	6.0
B4	1301	COPS	4.35	0.9	TSE-Co	2	–	200	100	7.1	3.7	5.7
B5	1301	COPS	8.7	1.9	–	0	–	200	100	7.0	3.6	9.1
B5b	1301	COPS	8.7	1.9	–	2	–	200	100	6.9	3.7	12.5
B6	1301	COPS	8.7	1.9	–	4	–	200	100	7.0	3.6	10.6
B10	1301	COPS	8.7	1.9	–	0	–	180	100	6.8	3.5	4.5
B8	1301	COPS	8.7	1.9	–	2	–	180	100	7.0	3.6	7.5
B7	1301	COPS	8.7	1.9	–	2	–	200	150	7.0	3.6	8.2
B9	1301	COPS	8.7	1.9	–	0	–	180	150	7.1	3.7	5.2
B11	20.3	COPS	8.7	1.9	–	0	–	160	100	7.2	3.6	8.0
B12	20.3	COPS	8.7	1.9	–	2	–	160	100	7.6	3.8	9.5
B13	20.3	COPS	8.7	1.9	–	4	–	160	100	7.1	3.6	6.1
B23	20.3	COPS	12.5	2.7	–	2	–	160	100	7.9	4.2	2.5
B24	20.3	COPS	25	5.4	–	2	–	160	100	7.9	4.0	2.7
B25	20.3	COPS	49.8	10.8	–	2	–	160	100	8.0	3.9	4.1
B31	20.3	COPS	8.7	1.9	Mini-	2	–	160	100	7.9	3.7	12.6
B29	1301	COPS	8.7	1.9	TSE-Cn	2	–	180	100	7.0	3.7	9.9
B32	1301	COPS	8.7	1.9	–	5	–	220	100	6.1	3.2	3.2
B33	1301	COPS	8.7	1.9	–	5	–	260	100	6.3	3.2	2.7
B15	1301	COPS	8.7	1.9	Co-dis-	–	–	60	–	8.1	4.2	17.5
B16	20.3	COPS	8.8	1.9	solution	–	–	60	–	8.8	3.9	6.3
PS1	1301	COPS	–	0	TSE-	–	5	195	200	–	–	–
PS2	1301	COPS	5.2	1.1	CORI	–	5	195	200	6.5	3.3	7.0
										6.5	3.4	15.0
PS3	1301	COPS	–	0	TSE-	–	5	195	200	–	–	–
PS4	1301	COPS	5.2	1.1	CORI+	–	5	195	200	6.4	3.2	6.4
					GP+					6.4	3.3	6.8
PS5	1301	C10A	2	1.2	EFM	–	5	195	200	4.3	1.5	5.7
					(gap = 15 μm)					3.8	1.5	2.0

The identification codes of the samples in column 1 are used in the text.

^a The experimental error of d_{001} measurements is ± 0.2 nm.

^b The error of m is about 5%.

temperature for 5 h. The oligomer (205 g of copolymer, prepared as described above) was dissolved in 2.2 l of THF in a 4 l round bottom flask. The solution was added drop-wise to the dispersed clay; a precipitate appeared immediately and the slurry was stirred at room temperature for 12 h. After stirring was stopped, the supernatant liquid was poured off, a fresh mixture of H₂O/THF (60/40) was added, and the slurry was stirred again for additional 12 h at room temperature. The slurry was filtered and the precipitate was air-dried for one day, and then in a vacuum oven at 40 °C for 48 h. The process yielded 224 g of COPS organoclay.



2.1.2. Polystyrenes

Two commercial PS were used in this work, namely PS1301, and PS20.3. Their properties are listed in Table 1.

2.2. Dispersion of organoclay in PS

Two methods have been used, melt compounding and solution blending. The procedures are outlined below and the tests results summarized in Table 2. Exfoliation means elimination of co-alignment of clay platelets, and their uniform dispersion in the matrix. This may be achieved only at low enough clay concentration (e.g. ≤ 1.1 wt% clay). Thus the attempts of exfoliation were carried out at 1–2 wt% of MMT.

2.2.1. Melt compounding

Melt compounding was carried out using one of the two TSE's: (1) the MiniLab co- or counter (cn)-rotating micro-compounder (mini-TSE from ThermoHaake). The device can be operated either using a single-pass, or (more frequently) recirculating the compound several times. (2) An industrial co-rotating, fully intermeshing TSE-CORI from Leistritz (TSE-34 mm, $L/D=40$) with high energy mixing screws.

Compounding 8.7 wt% of COPS (i.e. 1.89 wt% MMT) with of PS1301 in a mini-TSE was carried out at temperature $T=180$ – 260 °C; screw speed $N=100$ or 150 rpm; recycling (or recirculating) time $t_R=0$ – 300 s, with thermal stabilizer or without. Similarly, several samples were prepared with PS20.3, using the mini-TSE (with co- and counter-rotating screw configuration) at $T=160$ °C, $N=100$ rpm, and $t_R=0$ – 240 s, without stabilizer.

To verify the results, several PS1301/COPS compositions were also produced in TSE-34, with or without gear pump (GP), and an extensional-flow-mixer EFM (gap = 15 μ m). The details of PNC compounding with or without EFM are

available [24,25]. A side feeder was used for organoclays. For comparison, PS1301 was also compounded with C10A.

2.2.2. Solution blending

The two components, COPS and PS (with either high, or low M_w), were separately dissolved in toluene at room temperature (5 h with stirring). The solution of COPS in toluene was slightly milky, indicating sub-micron dispersion. The two solutions were combined in a stirred beaker at 60 °C, and during ca. 60 h the toluene partially evaporated. The concentrated solution was then cast into a thin film. The product was air dried, and then under vacuum at 60 °C for 48 h.

3. Characterization of nanocomposites

The COPS was analyzed for the presence of volatiles using the thermo-gravimetric analyzer (TGA). PS/organoclay compositions were characterized by X-ray diffraction (XRD), transmission electron microscopy (TEM), and scanning electron microscopy (SEM). In addition, dynamic flow behavior of PS/COPS nanocomposites at 160 or 180 °C, and mechanical properties (tensile, flexural and impact) at room temperature were determined—these will be discussed in part II of this paper [26].

3.1. TGA

The TGA measurements were carried out using Setaram Model TG96, with 10–12 mg COPS powder in a 100 μ l alumina crucible, under argon, increasing the temperature from 30 to 700 °C at a rate of 10 °C/min.

3.2. XRD

The XRD measurements were carried out in a Scintag X2 powder X-ray diffractometer with Cu K α radiation (wavelength $\lambda=0.15406$ nm). XRD scans were obtained at a scan rate of 0.3°/min. The specimens were prepared by compression molding at $T=180$ °C, using the compressive force of 5 ton (always using the same conditions and the same dimensions 13 \times 41 mm²) followed by re-molding on a cleaned glass slide to improve accuracy. The results are listed in Table 2.

The dominant interlayer spacing may be calculated from the XRD main diffraction peak position using Bragg's formula:

$$d_{00n} = \frac{n\lambda}{(2 \sin \theta)} \quad (1)$$

where, n is an integer, θ is the angle of incidence (or reflection) of X-ray beam, and λ is the X-ray wavelength. The thickness of the diffracting clay stack, t , was calculate from the XRD peak broadening from the formula credited to Scherrer [27]:

$$t = \frac{k\lambda}{(B_{1/2} \cos \theta_B)}; \quad k \cong 0.9 \quad (2)$$

where $B_{1/2} \cong \theta_1 - \theta_2$ is peak width at half peak height ($I_{\max}/2$), and $\theta_B \cong (\theta_1 + \theta_2)/2$. From Eq. (2), the number of clay platelets

per average stack with the interlayer spacing d_{001} can be calculated as $m = 1 + t/d_{001}$.

3.3. Electron microscopy

The PNC compounds with PS1301 or PS20.3 were compression molded at $T=180$ and 160 °C, respectively, using pressure $P=318$ – 1272 kPa for 4 min. The microstructure of PS/organoclay mixtures was examined in TEM and SEM. The specimens were prepared at room temperature using a Leica Ultracut FC microtome with diamond knife. The sections (nominal thickness of 70 nm) were transferred from water to 200-mesh Cu grids. The microtomed surface was observed under TEM (Hitachi H9000), or SEM (Hitachi S4700 FEGSEM).

4. Results

4.1. Characterization of COPS

4.1.1. Oligomer recovery (extraction)

To determine the molecular weight (MW) of the free oligomer and that of macromolecules bound to clay, two-step extraction was conducted. Firstly [28], COPS was mixed with toluene in centrifuge tubes for at least 5 h, and then centrifuged. The supernatant was decanted, dried, and tested in TGA—7 wt% inorganics was found. Secondly [29], the residue after toluene extraction was dried and a reverse cationic exchange reaction was employed using solution of 1 wt% LiCl in THF. The mixture was stirred overnight, centrifuged, and the supernatant was decanted, dried, and tested in TGA—32 wt% inorganics was found! Since the contaminating clay in the extracted materials could block the size exclusion chromatography (SEC) columns, the attempt to measure MW was abandoned.

4.1.2. Thermal gravimetric analysis

The ‘as received’ COPS was dried under vacuum at 60 °C for several weeks. TGA indicated the initial weight loss at $T \leq 150$ °C of ca. 1.4 wt% (Fig. 1) and the final weight loss of 78.3 wt%, thus MMT content in COPS was 21.7 wt%.

The glass transition temperature (T_g) was determined using a modulated differential scanning calorimeter (MDSC). The ground and dried COPS was scanned from 25 to 200 °C at the rate of 2 °C/min. As a result of the vacuum drying, T_g increased from 76 to 85 °C. Judging by this increase (and characteristic smell) the low temperature volatiles were mainly water and styrene.

4.1.3. XRD of COPS

Fig. 2 displays XRD scans for the COPS ground by hand or in a mechanical cryo-grinder. The scans show two peaks (stronger for the latter preparation), the first located at $2\theta \leq 1^\circ$ and the second at $2\theta \approx 2^\circ$. The former is named 1st peak and the latter is 2nd peak. The intensity of the 2nd peak is smaller than that of the 1st. From Eq. (1) the interlayer spacings for the hand ground COPS are $d_{001}=8.79$ and 8.83, and $d_{002}=4.42$ and

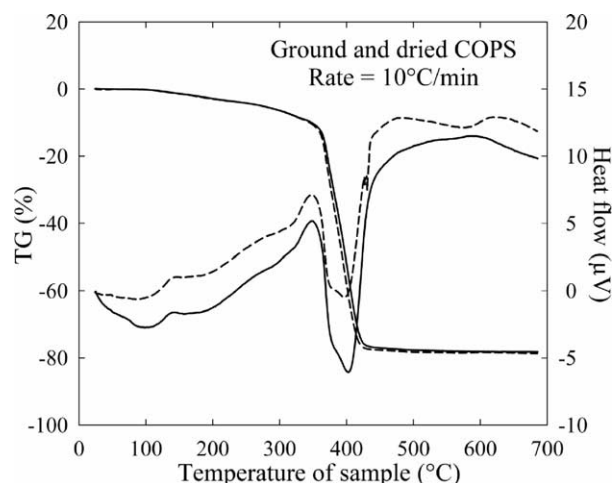


Fig. 1. TGA data for ground and dried COPS (two tests) heated at the rate of 10 °C/min. Mass of volatile matter ($T \leq 150$ °C)=1.4%; of medium volatile matter=76.9%; of non-volatile matter (MMT)=21.7%. The sample weight losses and heat flows are shown.

4.52 nm, giving the average value of $d_{001}=8.8 \pm 0.1$ nm. The interlayer spacings for cryo-ground COPS are $d_{001}=9.20$ and 9.82, and $d_{002}=4.75$ nm; hence the average $d_{001}=9.5 \pm 0.3$ nm. Since the main peak is located at small angle and prone to errors, the smaller interlayer spacing (8.8 ± 0.1 nm) is more reliable. For this peak Eq. (2) yields the number of clay platelets in the average stack $m \approx 7$.

4.1.4. TEM of COPS

The ground and dried COPS was compression molded at 100 °C at $P=281$ – 1125 kPa for 4 min and then microtomed using a diamond knife. Fig. 3 shows three ‘typical’ TEM micrographs of COPS at different magnification ($\times 80k$, $\times 120k$, and $\times 200k$). The platelets are mainly parallel to each other and the distance between them is about 10 nm (for 96 measures). Few, isolated platelets may be seen as well.

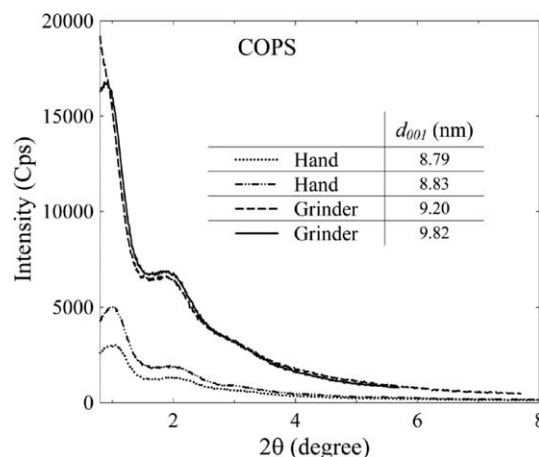


Fig. 2. XRD of COPS ground by hand or in a cryo-grinder. For better reproducibility, two tests were carried out using different samples.

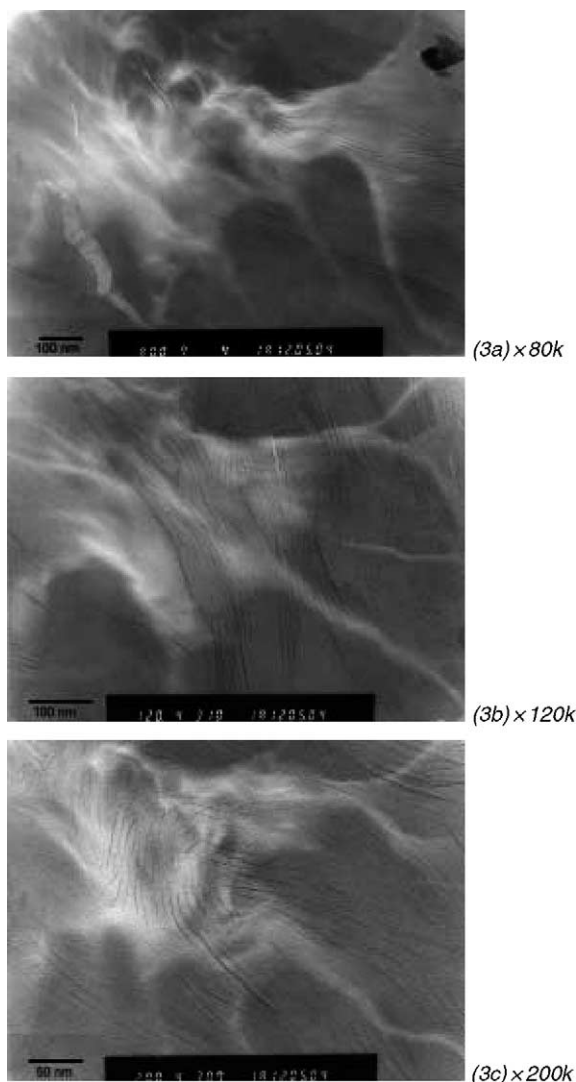


Fig. 3. TEM micrographs of COPS at magnification of $\times 80k$, $\times 120k$, and $\times 200k$.

4.2. Characterization of PS/COPS

4.2.1. XRD

The XRD scans of the PS20.3/COPS samples are shown in Fig. 4, and their interlayer spacings are listed in Table 2. The main interlayer spacing of the samples prepared by melt mixing in a co-rotating mini-TSE is $d_{001} = 7.3 \pm 0.2$ nm, i.e. smaller by 1.5 nm than that of neat COPS; the recirculating time had no effect on d_{001} . Samples prepared in the counter-rotating mini-TSE showed $d_{001} = 7.9$ nm; only the co-dissolution method managed to preserve the original COPS interlayer spacing of $d_{001} = 8.8 \pm 0.2$ nm. In the following text the samples are consistently identified by the code in column 1 of Table 2, viz. Bxy; PSz.

The calculated number of clay platelets per average stack for PS20.3/COPS mixtures, prepared by melt compounding and by dissolution, is $m = 9.0 \pm 0.5$ (6.1–12.6) and 6.3 ± 0.3 , respectively. Comparing these values to those obtained for neat COPS, $m \cong 7 \pm 0.3$, one must conclude that melt compounding resulted in a partial collapse of the interlamellar galleries,

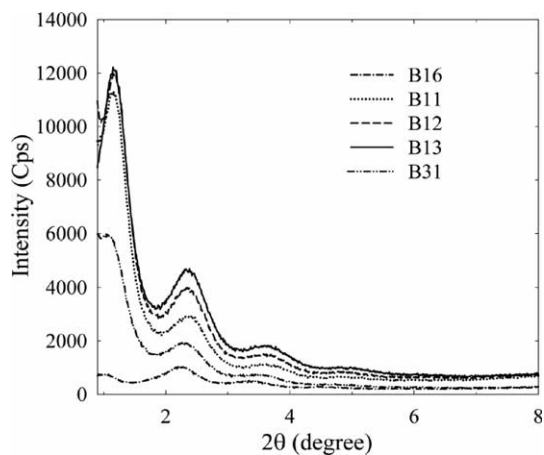


Fig. 4. XRD spectra of PS20.3 with 8.7 wt% of COPS PNC, prepared by melt compounding with different residence time, or by co-dissolution in toluene. Identification codes for the samples are listed in Table 2.

while co-dissolution slightly reduced the clay stacks, leaving the original interlayer spacing intact.

Similar XRD results were obtained for PS1301 with 8.7 wt% of COPS, (Table 2). The mixing without stabilizer (but under a blanket of N_2) was carried out using either co- and counter-rotating mini-TSE at screw speed $N = 100$ rpm, $T = 180$ °C, and the recirculating time of $t_R = 2$ min. The two screw configurations gave almost the same $d_{001} = 7.0 \pm 0.2$ nm, i.e. smaller than that obtained for systems with PS20.3. Co-dissolution of COPS with PS1301 resulted in $d_{001} = 8.2 \pm 0.2$ nm, which again is smaller than that obtained with PS20.3. However, the most significant is the increase of number of clay platelets per stack to $m = 17 \pm 1$.

The effect of compounding temperature was also investigated (Fig. 5). Samples were prepared using counter-rotating mini-TSE under a blanket of N_2 , at $N = 100$ rpm, $t_R = 2$ and 5 min, and $T = 180, 220$ and 260 °C. The $d_{001} = 7.0 \pm 0.2$ nm for the compound prepared at 180 °C was reduced to 6.1 and 6.3 nm for $T = 220$ and 260 °C, respectively, most likely caused by the thermal degradation of COPS.

Fig. 6 displays XRD results of PS/COPS prepared in a TSE-34, with (PS4) and without (PS2) a gear pump (GP) and the extensional flow mixer (EFM) [24,25]. The identification codes, PS2 and PS4 refer to Table 2. For comparison, scans of samples having the same compositions, but prepared in a mini-TSE, and that of neat COPS are also shown. For the PNC prepared, respectively, in a mini-TSE, TSE-CORI, and TSE + GP + EFM the interlayer spacing decreases from the original value for COPS of $d_{001} = 8.8$ nm to 7.0, 6.5 and 6.4 nm, respectively. Such a reduction of d_{001} may originate in the thermal degradation of the organoclay. Similar behavior was observed for PS/C10A systems—longer compounding and higher stresses resulted in more pronounced collapse of interlamellar galleries [19–21]. By contrast, compounding C10A with PS increased the original interlayer spacing from $d_{001} = 1.94$ to 4.3 ± 0.2 nm. Thus, it is evident that the interlayer spacing in PS/COPS is significantly larger than that in PS/C10A (the same compositions prepared under the same conditions). However, there are more clay platelets per

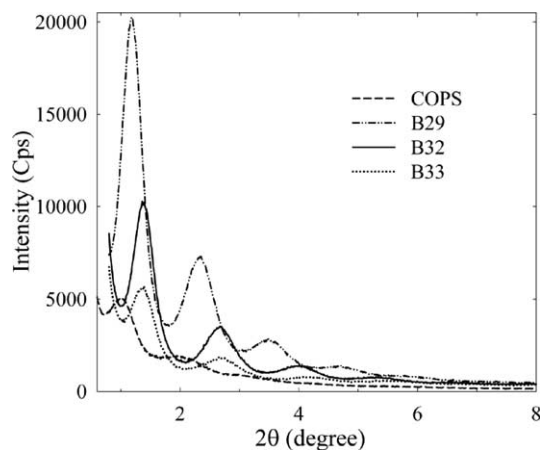


Fig. 5. XRD spectra of PS1301 with 8.7 wt% of COPS PNC, prepared by melt compounding in mini-TSE at different temperatures and residence times (Table 2).

PS/COPS stack than that in PS/C10A. Thus, the organoclay stack thickness for COPS and for C10A is about $t=63.4 \pm 0.6$ and 5.5 ± 0.3 nm, respectively.

4.2.2. SEM of PS/COPS

To validate the XRD results, samples were observed in a SEM and TEM. Figs. 7–11 presents the SEM micrographs of PS/PNC compounds prepared by four different methods.

Fig. 7 displays SEM micrographs of microtomed PNC prepared by co-dissolution of COPS and PS1301 (B15). Evidently, there are two domains: 91 wt% PS forms the matrix with dispersed domains of COPS. The same morphology, but with smaller COPS dispersed domains, was observed for the PNC prepared by co-dissolution of COPS in PS20.3 (B16).

The micrographs in Fig. 8 show the surface of melt compounded PS20.3/COPS (B12). Here COPS is well dispersed and distributed, but the particles are sufficiently large (10–15 platelets) to be evident in SEM. Figs. 9 and 10 display morphology of PS1301 with 5.2 wt% COPS, prepared in: TSE (PS2), and TSE + GP + EFM (PS4), respectively. The large number of elongated COPS domains illustrates the lack of

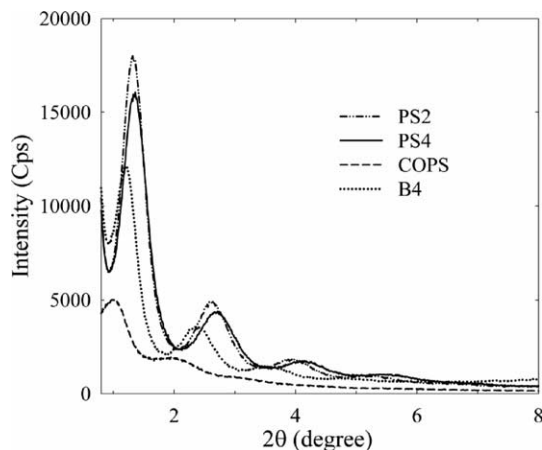


Fig. 6. XRD spectra of PS/COPS melt compounded in TSE + GP + EFM, or in mini-TSE (Table 2). Test specimens were prepared by injection molding. The spectrum of COPS is shown as a reference.

miscibility. A slightly better dispersion (larger number of COPS domains) was observed in PNC prepared using TSE-34 alone, confirming the XRD results. The micrographs in Fig. 11 present morphology of PS1301 containing 2 wt% C10A (PS5). The smaller number of larger particles evidences the poor dispersion of C10A in PS. In this Figure, particles up to 200 nm thick can be detected. Thus, the XRD result that gave $t=5.5$ nm provided information only about a local, atypical morphology of PS/C10A. When PS20.3 was used instead of PS1301, the dispersion was improved. Evidently, the degree of COPS agglomeration increases with the mechanical energy input, either as mechanically imposed stresses, or as increased matrix viscosity. It is noteworthy that compounding PA-6 or PP-based PNC's showed a reversed trend—an improvement of commercial organoclay dispersion when GP + EFM were added to TSE-34 compounding line [25].

4.3. TEM of PS/COPS

Fig. 12 shows a 'typical' TEM micrograph of PS20.3/COPS = 10:1 nanocomposites prepared by melt compounding. The SEM views of this material were presented in Fig. 8. Fig. 13 displays TEM micrograph of PS20.3/COPS = 10:1 PNC prepared by co-dissolution. The dispersion of COPS seems a bit better (smaller stacks; distance between platelets = 8.3 nm for 19 measures) than in Fig. 12 (larger stacks; distance between platelets = 7.4 nm for 30 measures). As inferred from XRD, the TEM images also show that COPS is not exfoliated. On a nano-scale, in melt-compounded or co-dissolved specimens there are stacks of 4–10 clay platelets, and few isolated platelets (e.g. in Fig. 12).

5. Discussion

As stated in the introduction, several reasons favor development of the mechanical compounding method for the manufacture of exfoliated PNC. This approach is already successful for polar and hydrophilic polymer-based PNC, and a large international efforts may soon offer viable melt compounding technology for the production of polyolefin based PNC. The key of the latter strategy involves compatibilization. Clay exfoliation in PS or other styrenics by compounding remains a challenge.

All melt compounding attempts of PS with commercial organoclays with or without compatibilizer failed to result in exfoliation. The only exfoliated PNC were produced using a reactive process, viz. by intercalating clay with vinyl-terminated ammonium ions and then initiating polymerization of styrene [4,5], or by introducing terminal ammonium group to an anionically polymerized PS, and then using it as a macro-intercalant [13].

During the last several years Wilkie and his collaborators developed a method of producing PNC's of a variety of polymers, including PS [22,30–33]. The method involved three steps [22], copolymerization of vinyl-benzyl chloride and styrene, followed by quaternization of an amine, and then ion exchange onto montmorillonite.

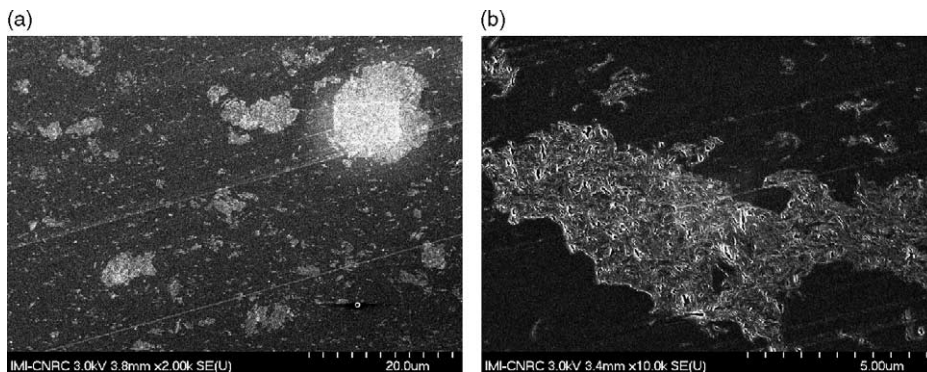


Fig. 7. SEM micrographs of microtomed samples of PS1301/COPS (B15) prepared by co-dissolution; magnification (a) $\times 2k$; (b) $\times 10k$.

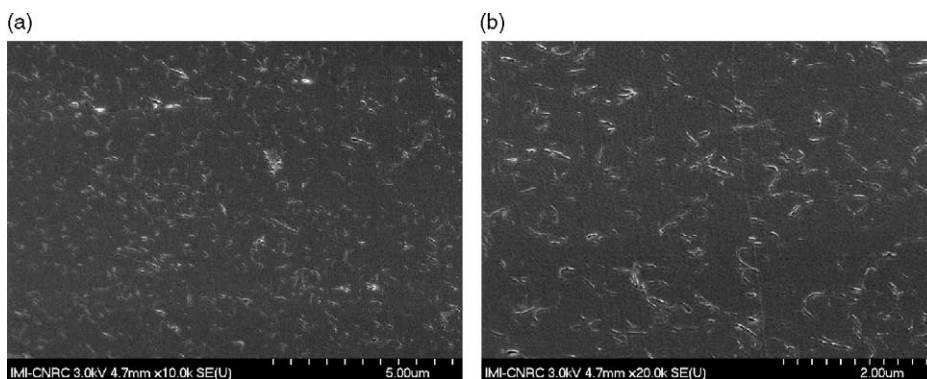


Fig. 8. SEM micrographs of microtomed samples of PS20.3/COPS (B12) prepared in the mini-TSE; magnification (a) $\times 10k$; (b) $\times 20k$.

Preparation of the COPS used in the present work followed a slightly simplified procedure. Thus, the first copolymerization step of styrene with 1.9 parts (per 100 parts of styrene) of vinyl-benzyl tri-methyl ammonium chloride, led directly to the oligomeric ammonium intercalant, capable to react with Na-MMT. Assuming random copolymerization, the resulting COPS has about 1.2 ammonium ions per macromolecule. Thus, statistically in the copolymer there should be 14% macromolecules without ammonium ion, 52% with one ion, and 34% of with at least two ammonium ions per macromolecule (assumption of 1.1 ammonium ions changes these numbers but little, viz. 17% without, 54% with 1, and 29% with ≥ 2 ammonium groups).

The molecular weight estimated from $T_g = 85^\circ\text{C}$ is within the range of 6 ± 1 kg/mol [34]. The Wyoming MMT used in COPS has the formula: $[\text{Al}_{3.263}\text{Mg}_{0.737}]^{-(0.737)}\text{Si}_8\text{O}_{20}(\text{OH})_4 + \text{H}_2\text{O Na}^{+0.737}$, ($M_o = 734$ g/mol), cation-exchange capacity $\text{CEC} = 1$ mequiv/g, surface area, $S = 750$ m²/g, density $\rho = 2500$ kg/m³, and that its platelets are rectangular: $1 \times 100 \times 500$ nm. Using these values one may find that there are about 75,000 Na^+ ions on the surface of one statistical platelet. The organic content in COPS is 78.3 wt%, thus statistically there are 45,000 intercalant molecules per clay platelet. However, since copolymerization results in about 1.2 ammonium ions per statistical macromolecule, the number of clay cations used in the reaction is 54,000 or 0.72 mequiv/g (i.e. ca. 28% clay

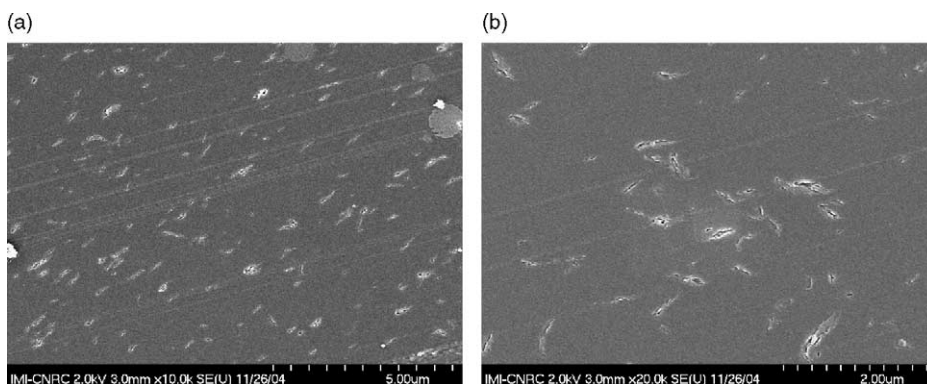


Fig. 9. SEM micrographs of microtomed samples of PS1301/COPS (PS2) prepared in the TSE; magnification (a) $\times 10k$; (b) $\times 20k$.

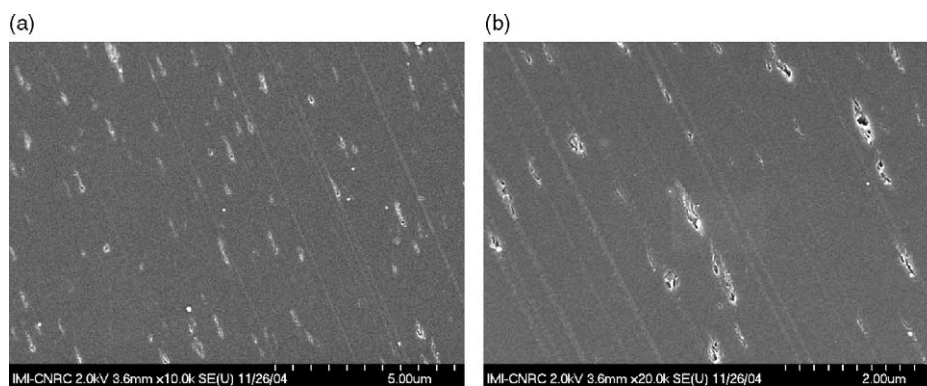


Fig. 10. SEM micrographs of microtomed samples of PS1301/COPS (PS4) prepared in the TSE+GP+EFM; magnification (a) $\times 10k$; (b) $\times 20k$.

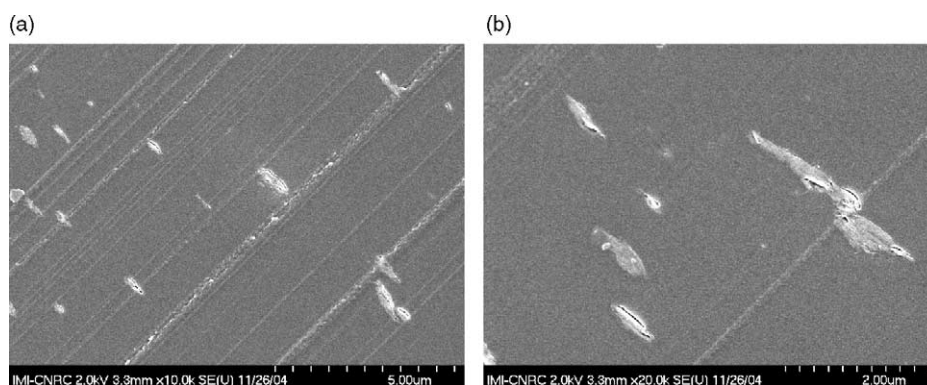


Fig. 11. SEM micrographs of microtomed samples of PS1301/C10A (PS5) prepared in the TSE+GP+EFM; magnification (a) $\times 10k$, (b) $\times 20k$.

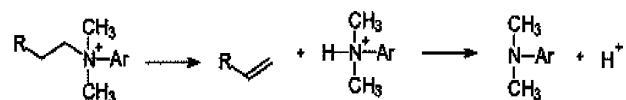
surface anions remain). Evidently, the intercalants able to react must have ammonium ion, thus in between the 54,000 intercalating oligomers there are 35,000 with a single, and 19,000 oligomers with at least two ammonium ionic groups. Most of the latter will react with anions belonging to the same clay platelet, but some will be able to react with another clay platelet, creating loosely bonded, organoclay aggregates—evident in Figs. 7–10.

5.1. Melt intercalation

Melt intercalation was carried out using three different compounders: two mini-TSE (co- and counter-rotating), as well as a 34 mm Leistritz TSE-34 with or without GP+EFM (the role of the gear pump, GP, is to provide the desired level of melt pressure for EFM) [35–37]. In the latter device, the extensional stresses are generated by flow through the convergent–divergent (C–D) channel with adjustable gap—the smaller the gap, the higher the extensional stresses. Thus, while in the mini-TSE the degree of mixedness depends on the melt recirculating time within the device, in TSE-34 with GP+EFM, that depends on the pressure and the C–D gap.

During melt compounding of PNC two processes simultaneously take place [19–21]. The first of these is the stress and strain controlled dispersion of organoclay platelets within the matrix, while the other is degradation. Several degradative processes are known to occur simultaneously, but for the PNC

compounding the most important is the thermal degradation of the ammonium intercalant, which follows the Hofmann elimination reaction [38]:



Experimentally, the onset of the Hofmann elimination occurs at about 150 °C [2,39]. The reaction results in the formation of a vinyl group, which in the presence of oxygen



Fig. 12. TEM micrograph of microtomed sample B12 prepared in co-rotating mini-TSE; magnification $\times 80k$ (for SEM see Fig. 8).



Fig. 13. TEM micrograph of microtomed sample B16 prepared by co-dissolution (Table 2); magnification $\times 80k$.

converts into peroxide, capable of initiating free radical chain scission that in turn accelerates the thermo-mechanical degradation of the matrix polymer. It is reasonable to expect that the strain-controlled distributive mixing will control the organoclay dispersion (provided that adequate stress is provided) [40–44], whereas high stress-controlled dispersive mixing with high local temperatures and pressures will lead to the intercalant degradation. Thus, in non-crosslinked systems some platelets may undergo expansion of the inter-gallery spacing, while others will suffer the opposite effect. Increased stress and pressure accelerates the latter process, while compounding under nitrogen slows it down. Of the four compounding systems used in this work, the co-rotating mini-TSE provided the mildest stress field, followed by the counter-rotating mini-TSE, TSE-34, and TSE-34 + GP + EFM (with small gap between the C–D plates).

5.2. Solution intercalation

To eliminate the possibility of degradation, and to improve the chances for good dispersion of COPS in PS, the co-solvent method was used. Surprisingly at first, the attempts at dissolution of COPS in toluene (or another good solvent for PS) [45] failed—the suspension remained turbid. Cast films from combined solutions of COPS with PS20.3 showed similar interlayer spacing of $d_{001} = 8.8 \pm 0.2$ nm, as that found for neat COPS. However, films cast from combined solutions of COPS and PS1301 had smaller interlayer spacing, $d_{001} = 8.2 \pm 0.2$ nm (Table 2). More significant is the number of clay platelets per stack—for compositions with PS20.3 and PS1301 $m = 6.3 \pm 0.3$, and 17 ± 1 , respectively.

Since the film preparation required $T \leq 60$ °C, and films with low molecular weight PS showed about the same d_{001} as that in COPS, thermal degradation is not the answer. Immiscibility between the lightly crosslinked COPS and PS is the source of problem. As the number of clay platelets per stack indicates, the immiscibility is far greater for the higher molecular weight PS1301 than that for PS20.3. In COPS galleries there is unbounded, soluble in toluene oligostyrene,

which may be extracted into the PS/toluene phase. Upon drying toluene is removed from the interlamellar galleries, which then shrink. From the change of d_{001} one can calculate that ca. $7 \pm 5\%$ of the intercalating oligomer was extracted, i.e., about 1/2 of the molecules produced without ammonium group.

5.3. Dispersion of clay platelets

The XRD results of neat COPS and its mixtures with PS are summarized in Table 2, where the interlayer spacing of two peaks at the smallest angles are listed. It is noteworthy that the interlayer spacing of the second peak is about 1/2 of the first, thus, in agreement with Bragg's Eq. (1), the first is assigned as d_{001} , whereas the second as d_{002} . This is important, since the data at small angles ($2\theta < 2$) are less reliable than those at higher angles. Accordingly, the values of the primary interlayer spacing could be calculated from both these peak positions.

The value of $d_{001} = 8.8 \pm 0.2$ nm was calculated for dried COPS, while the number of clay platelet per stack was $m \cong 7.0$ (for comparison, Cloisite[®] 10A has $d_{001} = 1.94$ nm, and $m \cong 1.9$). Slightly smaller spacing was observed in the PNC's prepared by the co-solvent method with PS1301: $d_{001} = 8.2 \pm 0.2$ nm. By contrast, melt compounding resulted in significant reduction of the interlayer spacing. Compounding in the mini-TSE's under a variety of mixing conditions resulted in $d_{001} = 7.0$ – 7.3 (± 0.2) nm for both PS grades. The only difference is for the PS20.3/COPS compound prepared with counter-rotating screw configuration ($d_{001} = 7.9 \pm 0.2$ nm). Compounding 5.2 wt% of COPS with PS1301 (i.e., ca. 1.2 wt% MMT) in a TSE-34 reduced d_{001} to about 6.5 ± 0.2 nm, and when TSE-34 + GP + EFM was used $d_{001} = 6.4 \pm 0.2$ nm was obtained. Thus, the XRD results show opposite tendency than expected—intensive melt compounding, instead of improving exfoliation resulted in reduction of the interlayer spacings.

In COPS/PS specimens, prepared either by co-dissolution or melt compounding, there are stacks of about 2–12 clay diffracting X-ray platelets, separated from each other by 6–8 nm. The parallel orientation of clay lamellae in stacks is less dependent on the long-range interactions than on the local concentration, which forces the platelets to pack tightly within the COPS domains. In the case of solution-prepared compound the average distance between platelets in the TEM micrographs of PNC is about 8.3 nm for 19 measures. Few isolated platelets (Fig. 13) may also be noted. In the case of melt-prepared nanocomposites, the TEM micrographs confirm the XRD results, showing a reduction of the gallery height in comparison to COPS (for 30 measures the average distance between platelets in the TEM micrographs is 7.4 nm). It is evident that two mechanisms are responsible for the reduction of the COPS interlayer spacing: (1) Extraction of unbounded oligostyrene from the interlamellar galleries (during the co-solvent procedure by toluene, and during melt compounding by molten PS), and (2) Hofmann elimination during the melt compounding at $T = 160$ – 200 °C, reinforced by the presence of high stresses in the compounding lines, e.g., in TSE + GP + EFM.

MMT intercalated with an aliphatic quaternary ammonium cations was found unstable at $T > 150\text{ }^\circ\text{C}$ [19–21,46–48]. In particular, Zhu et al. [31] studied the thermal stability of PS prepared with MMT intercalated with either ammonium or phosphonium cations. The data indicated that the former compound decomposed at $T > 200\text{ }^\circ\text{C}$, resulting in reduction of the interlamellar gallery height—a broad XRD peak was observed with $d_{001} = 1.58\text{ nm}$. Thus, when the processing temperature is high, thermal degradation of the intercalant causes reduction of the interlamellar gallery and re-aggregation of clay platelets. More recently, Kooli and Magusin measured XRD of a clay intercalated with tri-methyl hexadecyl ammonium (3MHDA) ions as a function of temperature [39]. Upon heating the interlayer spacing increased at $T = 50\text{--}150\text{ }^\circ\text{C}$, and then started to decrease—the onset of degradation was at $150\text{ }^\circ\text{C}$, and the most rapid collapse of interlamellar space was at $200\text{--}250\text{ }^\circ\text{C}$.

The XRD results for COPS compounded with PS are different from what has been observed for commercial organoclays with a polymer. In the latter cases upon mixing the original organoclay peak splits into two—one corresponding to a partial intercalation of the interlamellar galleries by matrix macromolecules, and the second resulting from the collapse of the interlayer spacing caused by degradation of the ammonium intercalant. For COPS only the second process is observed—there is no evidence of the matrix polymer migration into the organoclay galleries. This behavior reaffirms the immiscibility between COPS and the PS matrices.

5.4. Immiscibility

The immiscibility is evidenced by the SEM micrographs (Figs. 7–11) of the microtomed or fractured specimens. In all cases the presence of two-phases is evident. The micrographs of PNC prepared by the co-solvent method show the presence of dispersed domains, about $2\text{--}13\text{ }\mu\text{m}$ in size, larger for PNC with PS1301 than with PS20.3. The calculated fraction of these domains corresponds to the amount of COPS used in the experiments (ca. 8.8 wt%).

In polymer blends miscibility is rare, limited to systems with specific interactions [49], reflected in the negative value of the heat of mixing, $\Delta H_m < 0$. In blends the entropy of mixing (which mostly is responsible for miscibility in low molecular weight systems) is small, $\Delta S_m \approx 0$. In the case of COPS/PS mixtures at best $\Delta H_m = \Delta S_m \approx 0$ might be expected. However, for the configurational entropy to be zero, there must be equal probability of the PS macromolecules to be located anywhere within the system. This however is improbable, as PS macromolecules diffusing into the COPS interlamellar galleries would lose the configurational entropy. Such a loss could not be compensated by the entropy gain by the intercalant chains, as bonding of some intercalant molecules (with at least 2 ammonium groups) to adjacent clay platelets prevents gallery expansion.

Additional arguments for the immiscibility of COPS with PS are provided by the rheological studies, discussed in Part II of this paper [26].

6. Conclusions

The main objective of this work was to prepare exfoliated PNC with PS as the matrix. For this purpose, COPS organoclay with macromolecular intercalant was prepared. The preparation involved two steps: the free radical copolymerization of styrene with vinyl-ammonium compound, followed by Na-MMT intercalation.

Melt compounding of COPS with PS, instead of exfoliation engendered a two-phase dispersion. Furthermore, the interlayer spacing decreased with the increasing temperature and/or intensity of mixing. Next, the co-solvent method was used to engender a homogenous dispersion of clay platelets (at ca. 1.2 wt% of MMT) in PS matrix of low or high molecular weight. Again the attempt was unsuccessful. The electron microscopy provided direct evidence of two-phase structure.

The statistics of random copolymerization indicate that a significant proportion of copolymer molecules would have two ammonium groups, statistically capable of bridging the gap between adjacent clay platelets. The bridging creates a clay/oligostyrene network that is immiscible with PS. It is noteworthy to recall that in the macromolecular mixtures miscibility is a precarious—small configurational difference in two types of polymeric macromolecules (e.g., linear and branched polyethylene) is known to cause phase separation.

Acknowledgements

The authors gratefully acknowledge help from the technical staff of the NRCC/IMI, especially that from Chantal Coulombe, Florence Perrin, Yves Simard, and Manon Plourde.

References

- [1] Alexandre M, Dubois P. *Mater Sci Eng A* 2000;28:1–63.
- [2] Utracki LA. *Clay-containing polymeric nanocomposites*. 1st ed. Shawbury, Shrewsbury, Shropshire UK: RAPRA; 2004.
- [3] Qi R, Jin X, Nie J, Yu W, Zhou C. *J Appl Polym Sci* 2005;97:201.
- [4] Xu F, Qutubuddin S. *Mater Lett* 2000;42(1–2):12.
- [5] Tseng C-R, Wu J-Y, Lee H-Y, Chang F-C. *Polymer* 2001;42:10063.
- [6] Tseng C-R, Wu J-Y, Lee H-Y, Chang F-C. *J Appl Polym Sci* 2002;85:1370.
- [7] Uthirakumar P, Hahn YB, Nahm KS, Lee Y-S. *Eur Polym J* 2005;41:1582.
- [8] Zhong Y, Zhu Z, Wang S-Q. *Polymer* 2005;46:3006.
- [9] Khalil H, Mahajan D, Rafailovich M. *Polym Int* 2005;54:423 [see also 428].
- [10] Balazs AC, Singh C, Zhulina E. *Macromolecules* 1998;31:8370.
- [11] Kim K, Utracki LA, Kamal MR. *J Chem Phys* 2004;121:10766.
- [12] Hasegawa N, Okamoto H, Kawasumi M, Usuki A. *J Appl Polym Sci* 1999;74:3359.
- [13] Hoffmann B, Dietrich C, Thomann R, Friedrich C, Mülhaupt R. *Macromol Rapid Commun* 2000;21:57.
- [14] Lim YT, Park OO. *Macromol Rapid Commun* 2000;21:231.
- [15] Lim YT, Park OO. *Rheol Acta* 2001;40:220.

- [16] Wang H, Zeng C, Elekovitch M, Lee LJ, Koelling KW. *Polym Eng Sci* 2001;41:2036.
- [17] Uribe J, Kamal MR, Garcia-Rejon A, Utracki LA. Proceedings of the polymer processing society annual meeting, Guimarães, Portugal 2002.
- [18] Yoon JT, Jo WH, Lee MS, Ko MB. *Polymer* 2001;42:329.
- [19] Tanoue S, Utracki LA, Garcia-Rejon A, Tatibouët J, Cole KC, Kamal MR. *Polym Eng Sci* 2004;44:1046.
- [20] Tanoue S, Utracki LA, Garcia-Rejon A, Kamal MR. *Polym Eng Sci* 2004; 44:1061.
- [21] Tanoue S, Utracki LA, Garcia-Rejon A, Tatibouët J, Kamal MR. *Polym Eng Sci* 2005;45:827.
- [22] Su S, Jiang DD, Wilkie CA. *Polym Degrad Stab* 2004;83:333.
- [23] Kurata M, Tsunashima Y. In: Brandrup J, Immergut EH, Grulke EA, editors. *Polymer handbook*. 4th ed. New York: Wiley; 1999. p. VII [see also 1–83].
- [24] Tokihisa M, Yakemoto K, Sakai T, Utracki LA, Sepehr M, Li J, et al. Proceedings of the PNC-2005 international conference, Boucherville, QC, Canada 2005.
- [25] Utracki LA, Sepehr M, Li J. *Internl Polym Process* 2005; 20 (accepted for publication).
- [26] Sepehr M, Utracki LA, Zheng X, Wilkie CA. *Polymer* [the following paper].
- [27] Scherrer P. *Gött Nachr* 1918;2:98.
- [28] Meier LP, Shelden RA, Caser WR, Suter UW. *Macromolecules* 1994;27: 1637.
- [29] Yeh J-M, Liou S-J, Lin C-Y, Cheng C-Y, Chang Y-W. *Chem Mater* 2002; 14:154.
- [30] Wang J, Du J-X, Zhu J, Wilkie CA. *Polym Degrad Stab* 2002;77:249.
- [31] Wang D-Y, Wilkie CA. *Polym Degrad Stab* 2003;80:171.
- [32] Du J-X, Wang D-Y, Su S, Wilkie CA, Wang J-Q. *Polym Degrad Stab* 2004;83:29.
- [33] Jang BN, Wilkie CA. *Polymer* 2005;46:2933.
- [34] Fox TG, Loshaek S. *J Polym Sci* 1955;15:371.
- [35] Luciani A, Utracki LA. *Int Polym Proc* 1996;11:299.
- [36] Utracki LA, Luciani A. *Appl Rheol* 2000;10:10.
- [37] Utracki LA, Luciani A, Bourry DJJ, US Pat, 6,550,956, of Apr 22, to National Research Council of Canada; 2003.
- [38] Hofmann AW. *Justus Liebigs Ann Chem* 1851;78:253.
- [39] Kooli F, Magusin PCMM. *Clay Miner* 2005;40:233.
- [40] Dennis HR, Hunter DL, Chang D, Kim S, White JL, Cho JW, et al. *Polymer* 2001;42:9513.
- [41] Fornes TD, Yoon PJ, Keskkula H, Paul DR. *Polymer* 2001;42:9929.
- [42] Fornes TD, Yoon PJ, Paul DR. *Polymer* 2003;44:7545.
- [43] Fornes TD, Hunter DL, Paul DR. *Macromolecules* 2004;37:1793.
- [44] Shah RK, Paul DR. *Polymer* 2004;45:2991.
- [45] Brandrup J, Immergut EH, Grulke EA, editors. *Polymer handbook*. New York: Wiley; 1999.
- [46] Cho JW, Paul DR, Dennis HR, Hunter DL. Symposium on 'commercialization of nanostructured materials', Wyndham Miami Beach, Miami, FL 2000.
- [47] Zhu J, Morgan AB, Lamelas FJ, Wilkie CA. *Chem Mater* 2001;13:3774.
- [48] Delozier DM, Orwoll RA, Cahoon JF, Johnston NJ, Smith Jr JG, Connell JW. *Polymer* 2002;43:813.
- [49] Utracki LA. *Polymer blends handbook*. 1st ed. Dordrecht, Boston: Kluwer Academic Publishers; 2002.